*Int. J. Electrochem. Sci.*, 9 **(2014)** 2367 - 2378

International Journal of
ELECTROCHEMICAL
SCIENCE
www.electrochemsci.org

# Understanding the Mechanism of 2-mercaptobenzimidazole Adsorption on Fe (110), Cu (111) and Al (111) Surfaces: DFT and Molecular Dynamics Simulations Approaches

*I.B. Obot*[*], *Z. M. Gasem, S.A. Umoren*

Center of Research Excellence in Corrosion, King Fahd University of Petroleum and Minerals, Dhahran 31261, Saudi Arabia.
[*]E-mail: obot@kfupm.edu.sa

*Received:* 29 September 2013 / *Accepted:* 10 January 2014 / *Published:* 2 March 2014

Density functional theory (DFT) was carried out in order to establish which of the two forms of 2-mercaptobenzimidazole (2-MBI) (designated as 2-MBIthione and 2-MBIthiol) is actually responsible for the performance of 2-MBI as effective corrosion inhibitor for mild steel, copper, and aluminum. In this regard, geometrical parameters, electronic densities, global reactivity descriptors, electrostatic potential surfaces, and Mulliken charges on active atoms of the two tautomeric forms of 2-MBI on Fe (110), Cu (111) and Al (111) surfaces were computed and compared. The results indicate that the thione form of 2-MBI has the most reactive centers, has the highest electron donor capacity, lowest energy gap, highest fraction of electron transfered to the metal surfaces, carries a negative charge on its S atom and should be the most stable on the metal surfaces under investigation. According to molecular dynamics (MD) simulations the binding energy of the thione form of 2-MBI (2-MBIthione) on the metal surfaces follow the order: Fe (110) > Cu (111) > Al (111). This result indicates the effective inhibition of 2-MBI on steel corrosion when compared to aluminium and copper. This study has provided an important insight that will assist in designing novel and effective inhibitors based on 2-mercaptobenzimidazole scaffold for the control of both abiotic and microbially- influenced corrosion (MIC) for metals and alloys.

**Keywords:** Adsorption, DFT, 2-mercaptobenzimidazole, Molecular Dynamics Simulations.

## 1. INTRODUCTION

The study of material corrosion process and the adsorption mechanism of organic inhibitors on metal and alloys is an important area of research which has theoretical and practical relevance in academic and industrial environments [1]. Many efficient corrosion inhibitors are organic compounds rich in hetero-atoms such as nitrogen, oxygen, sulfur and π-bonds. It has been reported that organic

inhibitors bearing both nitrogen and sulphur atoms on the same molecular structure are more effective than inhibitors having only nitrogen atom [2]. It is generally accepted that corrosion inhibition efficiency of organic compounds is related to their adsorption properties [3-5]. The adsorption of these molecules depend mainly on certain physicochemical properties of the inhibitor molecule such as, functional groups, steric factor, aromaticity, electron density at the donor atoms, p-orbital character of donating electrons, electronic structure of the molecules and the strength of interaction between the inhibitor and the metal surface [6-8].

Density functional theory (DFT) has become an attractive theoretical method, because it gives exact, basic, and vital parameters for small and even complex molecules at lower cost [9]. Moreover by applying DFT methodology, we can understand reactivity behavior in terms of hard and soft acid/base (HSAB) theory which can provide a systematic way for analyzing and predicting inhibitor/surface interaction [10]. However, it has been observed that it is difficult to acquire all the necessary information about the binding strength between organic inhibitor and bulk metal surface which is pertinent in estimating inhibitor performance using DFT only [11].

The above deficiency can be solved by using molecular dynamic simulations, which in recent times have been used to study the interaction between corrosion inhibitors and metal surfaces [12-14]. MD simulations gives information at the molecular level on the adsorption of the inhibitor molecules on corroding metal surfaces. Furthermore, vital information on the conformation of inhibitors adsorbed onto metal surfaces and the interaction energy between them can be readily obtained [15]. Thus, MD simulations methodology can provide powerful insights into the design of inhibitor systems with superior properties and differences in inhibition efficiency among homologues inhibitors (inhibitors bearing similar structures) can be systematically explained.

Benzimidazoles form a family of well known corrosion inhibitors for different metals and alloys in different aqueous environments [16, 17]. They consist of benzene and imidazole rings. One of the most important derivatives of this family is 2-mercaptobenzimidazole (2-MBI). Its corrosion inhibition potentials on metals and alloys has been documented [18, 19]. DFT studies on the interaction between benzimidazole with Fe (110), Cu (111) and Al (111) has been reported [20]. In the same vein, density functional theory study of imidazole, benzimidazole and 2-mercaptobenzimidazole adsorption onto Cu (111) surface has recently been reported [21]. It was concluded from the studies that the preferred adsorption mode of 2-mercaptobenzimidazole on Cu (111) is when the neutral form of the inhibitor is parallel to the metal surface. However, information on the actual tautomeric form of 2-mercaptobenzimidazole (2-MBI) responsible for the adsorption and the mechanism of its interaction on different metals has not been investigated to be best of our knowledge. This is the main objective of the present study.

## 2. COMPUTATIONAL DETAILS

All geometry optimizations and quantum chemical calculations were performed using density functional theory (DFT). The Becke's Three Parameter Hybrid Functional using the Lee-Yang-Parr correlation functional theory (B3LYP, [22]) was selected for the calculations. Calculations were done

using the 6-31G (d,p) basis set in the gas phase. Molecular properties estimated include the highest occupied molecular orbital (HOMO) energies, lowest unoccupied molecular orbital (LUMO) energies and other molecular properties derived from HOMO and LUMO energies. All optimization calculations were done using the Gaussian 03 program [23].

MD simulations of the interaction between inhibitor molecules and the metal surfaces was carried out using Materials Studio 6.0 (from Accelrys Inc) [24, 25]. To construct the interaction model, the Fe, Cu and Al cells were optimized, followed by a four-step model construction: (i) cleaving the surface along different planes, then relaxing the surface; (ii) building the 2D surface into a super cell; (iii) and adding a vacuum slab above the metal surfaces to build a 3D cell, and setting the vacuum thickness as 30A˚ ; (iv) then placing the energy minimized inhibitor molecule onto a proper position on the surface, and ensuring that the whole molecule is inside the vacuum slab – this position, called initial position, is relatively arbitrary, and several initial positions are required when calculating the averaged interaction energies. Calculations were carried out, using the COMPASS force field and the Smart algorithm, in a simulation box with lattice parameters of 29.78 × 24.82 × 28.18; 23.00 × 23.00 × 38.43; 25.77 × 25.77 × 39.43 all in Angstrom ($A^o$) for Fe (110); Cu(111); and Al (111) respectively, with a super cell (9 x 9) containing the Fe, Cu and Al surfaces. After constructing the 3D interaction models, dynamics simulations was performed. First, the model was equilibrated in NVT ensemble (i.e. canonical ensemble) at 298.0 K with a time step of 0.1 fs and a simulation time of 50 ps. 50 production runs were performed on the low potential energy frames with NVT ensemble at 298.0 K using Nose thermostat. We have neglected solvent and charge effects in all our simulations and performed the calculations at the metal/vacuum interface. Although this is clearly an oversimplification of the factual situation, it is adequate and has been used by many researchers in illustrating the differences in the adsorption behaviour of organic molecules on metal surfaces and to rationalize experimental findings [26, 27].

The binding energy of 2MBI thione and 2MBI thiol molecules on the metal surface was estimated following the equation [28]:

$$E_{binding} = E_{total} - (E_{surface} + E_{mol}) \quad (1)$$

where $E_{total}$ is the total energy of the surface and inhibitor, $E_{surface}$ is the energy of the surface without the inhibitor molecule, and $E_{mol}$ is the energy of the inhibitor molecule without the surface. Studies have shown that the adsorption energy of the inhibitors on the metal surface correlates with the inhibition efficiency exhibited by inhibitors [29].

## 3. RESULTS AND DISCUSSION

### *3.1. Tautomeric and optimized geometrical structures of 2-MBI*

2-mercaptobenzimidazole (2-MBI) may exist as 2-MBI thione and 2-MBI thiol tautomers as shown in Scheme 1. It has been reported that 2-MBI exists predominantly in the thione form in the solid and in polar solvents such as ethanol, water, and dimethyl sulfoxide [30]. One of the driving forces favouring the 2-MBI thione tautomeric form is believed to be that the N-H bond forms a

stronger hydrogen bond with the solvent or another 2-MBI molecule than the S-H bond [30]. As an imidazole-thiol, 2-MBI has two N atoms and one S atom and they can synergistically or individually contribute to its binding to metals surfaces. The conversion from one tautomeric form to another of 2-MBI is important from the point of view of structural chemistry.

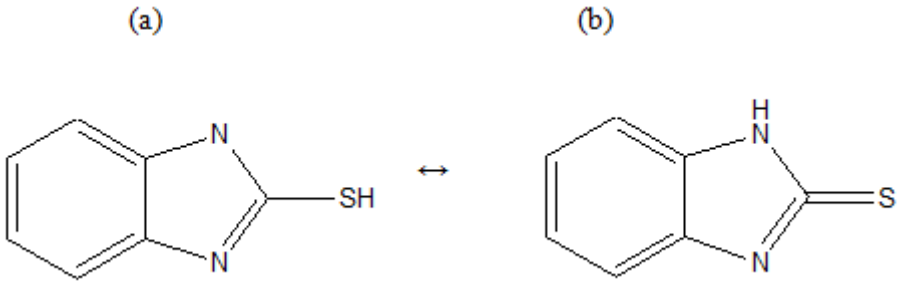


**Scheme 1.** (a) The thiol and (b) thione forms of 2-MBI

**Table 1.** Selected bond lengths (in angstroms) and bond angles (in degrees) of 2-MBI thione and 2-MBI thiol forms of 2-mercaptobenzimidazole (2-MBI) calculated using B3LYP/6-31G (d,p) level.

| Parameters | 2-MBI thione | 2-MBI thiol | Exp[31] |
|---|---|---|---|
| C1-C7 | 1.389 | 1.388 | 1.389 |
| C2-C4 | 1.390 | 1.399 | 1.391 |
| C2-N9 | 1.389 | 1.392 | 1.389 |
| C8-N7 | 1.376 | 1.378 | - |
| C8-N9 | 1.376 | 1.307 | 1.365 |
| C8-S10 | 1.666 | 1.769 | 1.684 |
| N7-C8-S10 | 127.70 | 120.14 | - |
| N9-C8-S10 | 127.70 | 125.92 | 127.21 |
| C1-N7-C8 | 111.60 | 106.52 | 111.01 |
| C2-C4-N9 | 132.60 | 129.75 | 132.02 |
| C2-C4-C6 | 117.27 | 118.01 | 116.32 |

B3LYP/6-31G(d,p) calculations were performed on the two tautomeric forms of 2-MBI. Calculated geometric parameters are listed in Table 1 along with the experimental data. The crystallography study [31], shows that the thione form is predominantly present. According to published data by Ravikumar et al, [31], 2-MBI thione molecule is bisected by the crystallographic mirror plane with atoms C8-S10 lying in this plane. The C8-S10 bond length of 1.684 $A^o$, determined experimentally possesses 58% SCF π-bond character [31]. This value of bond length is confirmed theoretically in the case of 2-MBI thione which is closer to the experimental result than the 2-MBI thiol form (Table 1). The bond lengths and bond angles obtained experimentally for 2-MBI agree well with those computed using DFT, but the slight differences in bond lengths and angles between the two forms of 2-MBI may be attributed to the migration of hydrogen atom and the delocalization of electron

density during the tautomeric formation. However, the molecules are largely planar.

*3.2. Frontier molecular orbitals and global reactivity indices*

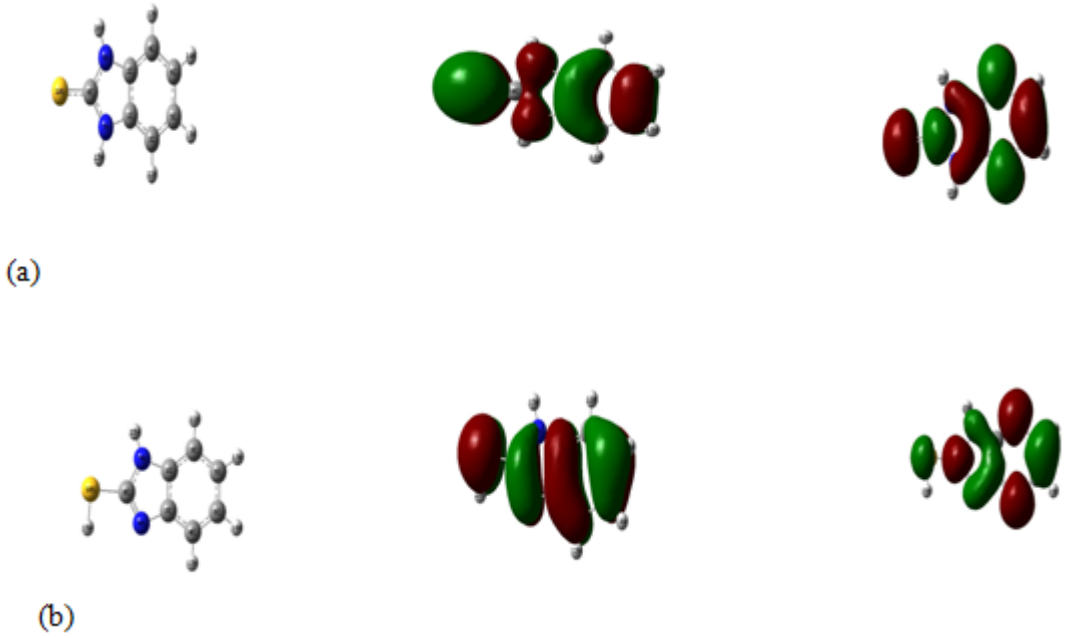


**Figure 1.** (a) Optimized structure, HOMO and LUMO orbitals of 2-MBI thione; (b) optimized structure, HOMO and LUMO orbitals of 2-MBI thiol.

In order to understand the different bonding abilities of the two forms of 2-MBI onto a metal surface at the atomic level, quantum chemical calculations was employed to obtained some electronic properties and orbital information. The optimized structure, HOMO and LUMO orbitals of 2-MBI tautomers are shown in Figs. 1(a) and (b). Similarly, the calculated quantum chemical properties for the most stable conformations of 2-MBI thione and 2-MBI thiol calculated using B3LYP/6-31G (d,p) level is presented in Table 2. According to frontier molecular orbital theory (FMO) of chemical reactivity, the formation of a transition state is due to an interaction between frontier orbitals (HOMO and LUMO) of reacting species [32]. The energy of HOMO and LUMO is often associated with the electron donating ability and electron accepting ability. The organics does not only donate electrons to the unoccupied d- orbital of the metal ion (in case of transition metal) but can also accept electrons from the d-orbital of the metal (in case of transition metal) leading to the formation of a feed-back bond [33]. Thus, the binding ability of organics to the metal surface increases with increase in energy of the HOMO and decrease in the value of energy of the LUMO. The energy gap, $\Delta E$, is an important parameter which indicates the reactivity tendency of organics towards the metal surface [34]. As $\Delta E$ decreases, the reactivity of the molecule increases leading to an increase in adsorption onto a metal surface. A molecule with low energy gap is more polarizable and is generally associated with high chemical reactivity and low kinetic stability. Thus, $\Delta E$, has been used in literature to characterize the

binding ability of organics to the metal surface. [35]. The dipole moment ($\mu$ in Debye) is another important reactivity parameter than has been frequently used to understand the distribution of charges on the atoms in a molecule. The high value of dipole moment has been reported to increase the adsorption between an organics and a metal surface [36].

**Table 2.** Calculated quantum chemical properties for the most stable conformations of 2-MBI thione and 2-MBI thiol calculated using B3LYP/6-31G (d,p) level.

| Properties | 2-MBI thione | 2-MBI thiol |
|---|---|---|
| Total Energy (Ha) | -778.09 | -778.06 |
| $E_{HOMO}$ (eV) | -5.46 | -5.83 |
| $E_{LUMO}$ (eV) | -0.84 | -0.37 |
| $\Delta E$ (eV) | 4.62 | 5.46 |
| $\mu$ (D) | 4.75 | 2.25 |

As can been seen in Table 2, the total energy of the thione form is slightly lower than that of the thiol form which indicates that 2-MBI thione is more stable than 2-MBI thiol. Also from Table 2, 2-MBI thione has a higher $E_{HOMO}$ and a lower $E_{HOMO}$ than 2-MBI thiol which indicate that the electron donating and accepting ability of 2-MBI thione is higher than that of 2-MBI thiol. The lower value of energy gap, $\Delta E$, computed for 2-MBI thione corresponds to a more stable adsorption layers of the organics on the metal surface. The higher value of the dipole moment as computed in Table 2 for 2-MBI thione, confirms its higher adsorption ability to the metal surface than the 2-MBI. This is because the volume of the molecule and its contact area to the metal surface increases with higher dipole moment.

The HOMO and LUMO orbitals of 2-MBI thione and 2-MBI thiol forms of 2-MBI are also presented in Fig 1. From the molecular orbital distribution it can be seen that the HOMO and LUMO orbitals are localized on the whole structure but with a higher lobe around the S atom in 2-MBI thione than in 2-MBI thiol form. This shows the importance of S atom in the bonding ability of 2-mercaptobenzimidazole (2-MBI) on the metal surface.

### *3.3. Mulliken population distribution and molecular electrostatic potential surfaces*

Mulliken population distribution is commonly used in quantum chemical calculations to establish the active centers of organic molecule responsible for interaction with metals. It has been documented that the more negative the atomic charges of the adsorbed center, the more easily the atom donates its electron to the unoccupied orbital of the metal [37]. The molecular electrostatic potential, MEP, is related to the electron density and is a very useful descriptor in determining the sites for electrophilic and nucleophilic reactions as well as hydrogen bonding interactions [38].

Figs. 2 (a) and (b) show the Mulliken charge distributions and the molecular electrostatic potential map of 2-MBI thione and 2-MBI thiol ( red=negative charge and blue = positive charge). It is clear from Figs. 2(a) and (b) that the two N atoms carries high negative charges whereas some ring

carbon atoms (benzo carbons) carries substantial negative charges. The biggest difference is that whereas the S atom of the 2-MBI thione carries a negative charge, the S atom of the 2-MBI thiol carries a positive charge. This make the 2-MBI thiol unstable and less reactive when compared with 2-MBI thione. To predict reactive sites for electrophilic and neucleophilic attack, the MEP at the B3LYP/6-31G(d,p) optimized geometry was plotted. The negative (red and yellow) regions are related to electrophilic centers whereas the positive (blue) regions to nucleophilic centers. As can be seen from Fig. 2, that the two molecules has many possible reactive centers. Negative charges are located over the two N atoms, the C atoms of the benzene rings and much more at the S atom. However, the S atom of the 2-MBI thione carries more negative charges (more red colour) when compared to 2-MBI thiol which carries positive charges (blue colour). Thus, the negative charge on the S atom present in 2-MBI thione is the primary reason why its interaction with the metal surface is expected to dominate over that of 2-MBI thiol.

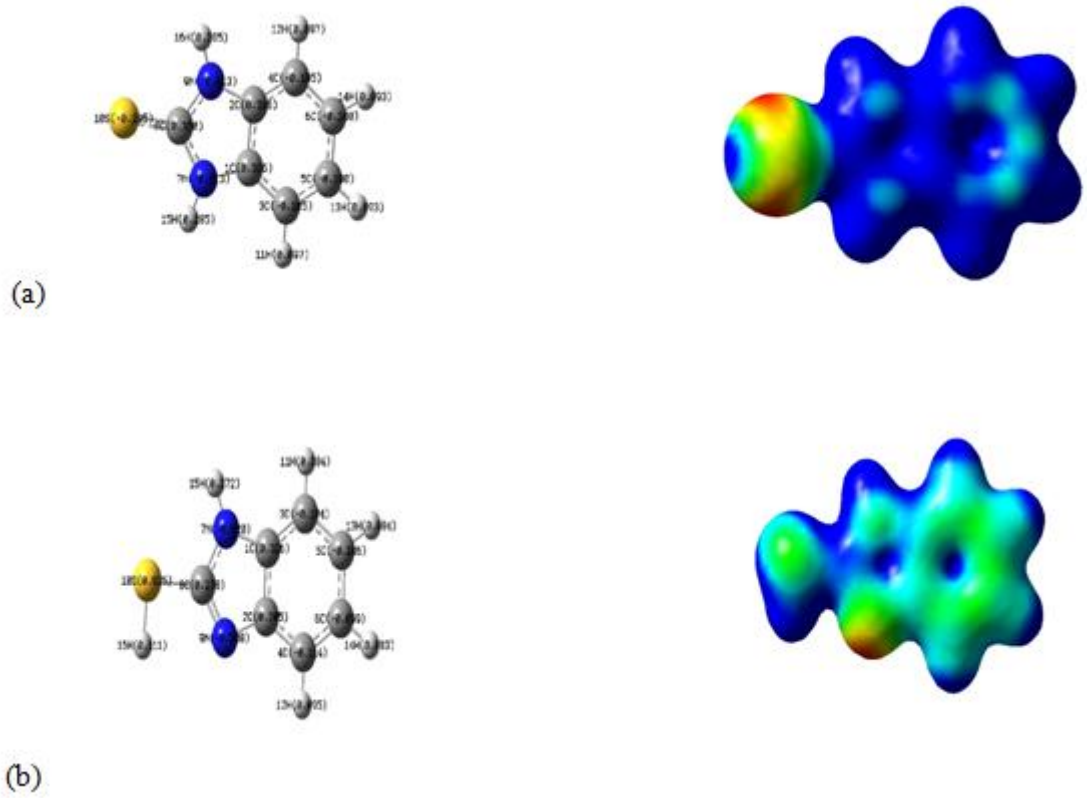


**Figure 2.** (a) Charge distribution and electrostatic potential map of 2-MBI thione; (b) Charge distribution and electrostatic potential map of 2-MBI thiol.

*3.4. Molecular dynamic simulations*

Recently, molecular dynamics (MD) simulations are performed to study the interaction of several corrosion inhibitors with metal surfaces [39, 40]. Results obtained from those studies indicate that molecular dynamics simulations can provide insights into the design of inhibitor systems with

superior properties, and the interaction energy between organic molecule and metal surface given by molecular dynamics simulations can interpret the difference of inhibition efficiency between organic inhibitors. In order to understand the adsorption mechanism of interaction of 2-MBI thione, the most stable form of 2-mercaptobenzimidazole with iron, aluminium and copper metals, MD simulations was carried out.

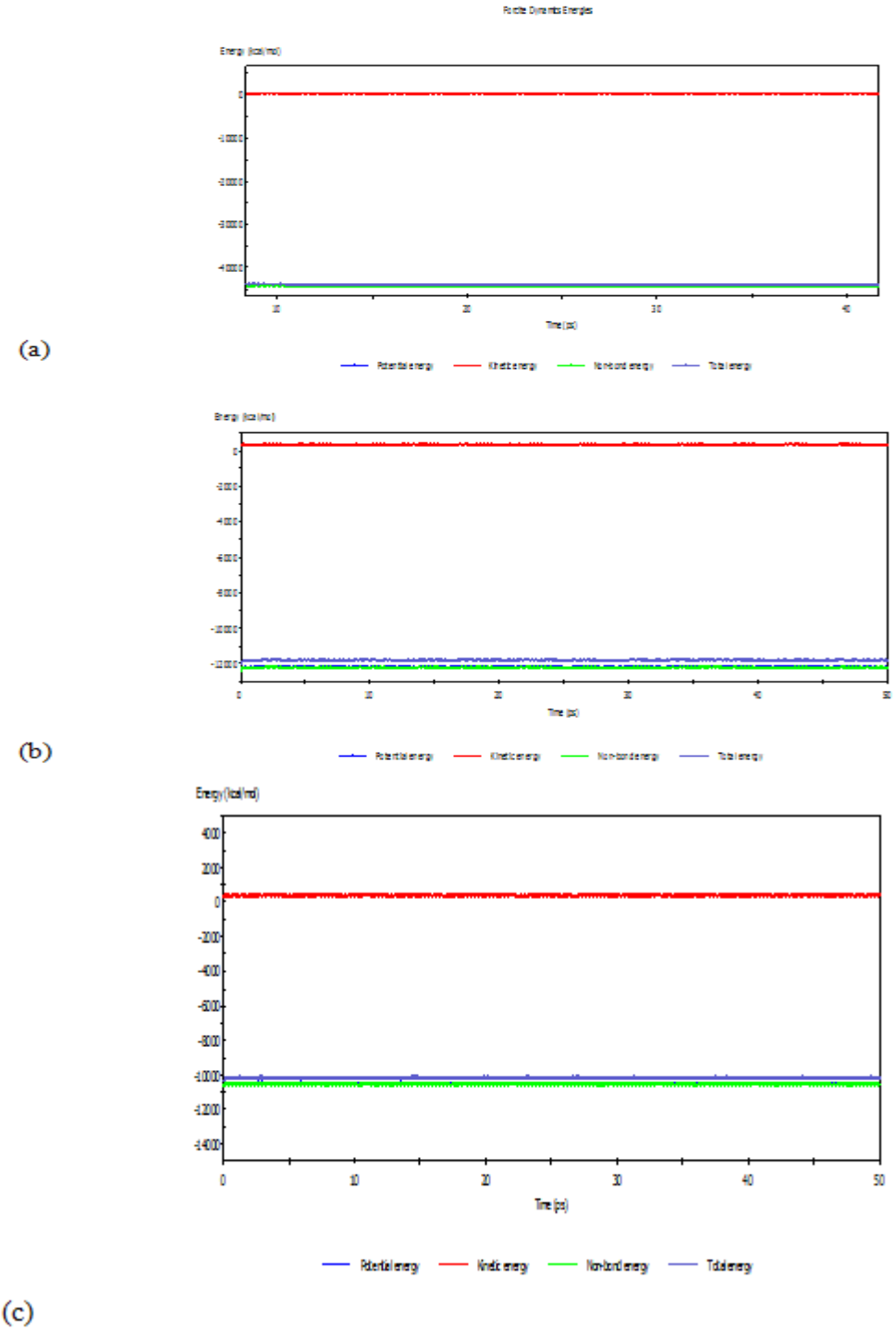


**Figure 3.** Energy fluctuation curves for the equilibrium adsorption of 2-MBI thione on (a) Fe (110) (b) Cu (111) and (c) Al (111) surfaces.

The simulation studies were design to predict the binding strength of 2-MBI thione with Fe, Cu and Al surfaces in order to determine the adsorption strength of the molecule on these different metals. 2-MBI thione has several potential binding sites as revealed in the quantum chemical calculation earlier discussed. The active sites include the S atom, the two N atoms and several π-electrons. These atoms and π-systems can bind to the metal surfaces. Thus 2-mercaptobenzimidazole can act as corrosion inhibitor. MD simulations were performed to study the adsorption behaviour of 2-MBI thione on Fe (110), Cu (111), and Al (111) surfaces. When the energy of the systems containing 2-MBI thione adsorbed on Fe (110), Cu (111), and Al (111) reaches equilibrium (Figs. 3), the values of $E_{total,}$ $E_{surface}$ and $E_{mol}$ were subsequently evaluated from single point energy calculations. The $E_{binding}$ between Fe (110), Cu (111) and Al (111) surfaces with 2-MBI thione can be obtained according to Equ.(1). The close contacts between the molecules and the metal surfaces as well as the best equilibrium adsorption configuration for the compounds are depicted in Fig. 4. The calculated $E_{interaction}$ and $E_{binding}$ values for the different systems are given in Table 3.

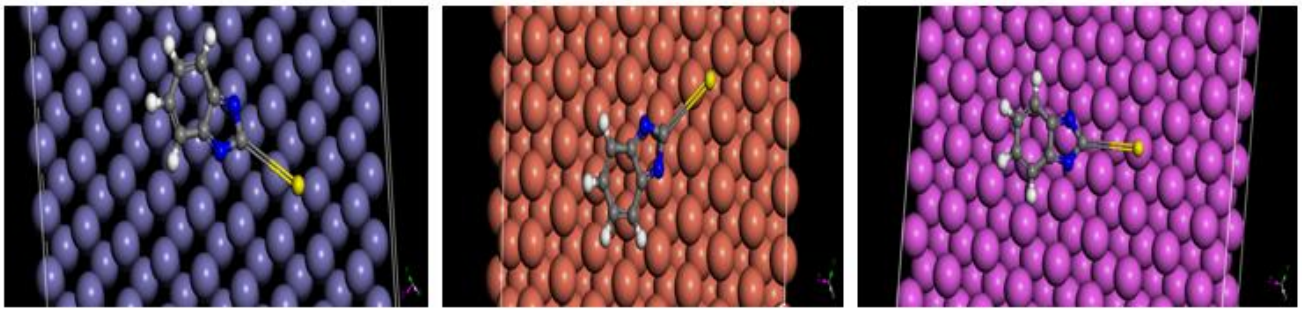

A B C

**Figure 4.** Equilibrium adsorption configurations of 2-MBI thione on (a) Fe (110) (b) Cu (111) and (c) Al (111) surfaces obtained by molecular dynamics simulations.

**Table 3.** Interaction and binding energies of 2-MBI thione adsorbed on Fe (110), Cu (111) and Al (111) surfaces.

| Systems | $E_{interaction}$ (kJ mol$^{-1}$) | $E_{binding}$ (kJ mol$^{-1}$) |
|---|---|---|
| Fe (110) + 2-MBI thione | -191.84 | 191.84 |
| Cu (111) + 2-MBI thione | -126.03 | 126.03 |
| Al (111) + 2-MBI thione | -71.95 | 71.95 |

It can be seen that the 2-MBI thione adsorbed on the metal surfaces with a flat orientation. The formation of the flat orientation can be ascribed to the relatively equal distribution of populations of HOMO and LUMO on the whole molecules. This ensures high adsorption strength and interaction energy which makes 2-MBI efficient corrosion inhibitor for the metals.

Results obtained from Table 3 shows that the interaction energy between 2-MBI thione and the three metal surfaces were all highly negative and therefore spontaneous adsorption is expected. It has been documented that the more negative the interaction energy between an organic molecule with a metal surface is, the stronger is the binding energy and the more stable is the interaction [41, 42]. It is thus clear from this study that 2-MBI thione is more stable on the three metal surfaces. The binding strength of 2-MBI thione with the different metal surfaces follows the order: Fe > Cu > Al. The adsorption mechanism of 2-mercaptobenzimidazole (2-MBI) with the different metal surfaces studied can be attributed to the strong interaction between the S atom, two N atoms and several π-electrons. These atoms can offer electron densities to the unoccupied-orbitals of Fe, Cu, and Al to form coordinate bonds, and the anti-bonding orbitals of π-electrons in the imidazole and benzene moiety present in 2-MBI can also accept the electrons from the empty-orbitals of the metals to form feedback bonds. This interaction is stronger for Fe than Cu and Al.

## 4. CONCLUSIONS

Density functional theory (DFT) and molecular dynamics (MD) simulations have successfully been used to gain some insights into chemical reactivity and mechanism of corrosion inhibition of 2-mercaptobenzimidazole (2-MBI) on Fe, Cu, and Al surfaces at the molecular level. DFT results show that the thione form of 2-MBI designated as 2-MBI thione is more reactive and stable than the 2-MBI thiol form. The active reaction sites of 2-MBI thione with the metal surfaces are S atom, the two N atoms on the imidazole moiety and the π-electrons on the system. MD simulation showed that 2-MBI thione binds spontaneously to the three metal surfaces investigated. This study has provided an important insight that will assist in designing novel and effective inhibitors based on 2-mercaptobenzimidazole derivatives.

ACKNOWLEDGMENTS
The authors gratefully acknowledged the support of High Performance Computing (HPC) Center, King Fahd University of Petroleum and Minerals (KFUPM) Saudi Arabia for making the Material Studio software available. Center of Research Excellence in Corrosion at KFUPM is also acknowledged for encouragement.

## References

1. I.B. Obot, N.O. Obi-Egbedi, *Corros. Sci.* 52 (2010) 198.
2. I.B. Obot, N.O. Obi-Egbedi, *Corros. Sci.* 52 (2010) 657.
3. I.B. Obot, N.O. Obi-Egbedi, S.A. Umoren, *Corros. Sci.* 51 (2009) 276.
4. M.M. Kabanda, L.C. Murulana, M. Ozcan, F. Karadag, I. Dehri, I.B. Obot, E. E. Ebenso, *Int. J. Electrochem. Sci. 7* (2012) 5035.
5. I. B Obot, N. O. Obi-Egbedi, *Curr. Appl. Phys.* 11 (2011) 382.
6. I.B. Obot, N.O. Obi-Egbedi, *Corros. Sci.* 52 (2010) 282.
7. I.B. Obot, N.O. Obi-Egbedi, N.W. Odozi, *Corros. Sci.* 52 (2010) 923.

8. I.B. Obot, N.O. Obi-Egbedi, *Mater. Chem. Phys.* (2010) 325.
9. P. Geerlings, F. De Proft, W. Langenaeker, *Chem. Rev*. 103 (2003) 1793.
10. W. Yang, R.G. Parr, *Proc. Natl. Acad. Sci*. 82 (1985) 6723.
11. I. Lukovits, E. Kalman, F. Zucchi, *Corrosion* 57 (2001) 3.
12. I. B. Obot, E. E. Ebenso, N. O. Obi-Egbedi, A. S. Afolabi, Z. M. Gasem, *Res. Chem. Intermed.* 38 (2012) 1761.
13. K.F. Khaled, *Electrochim. Acta 53*, (2008) 3484.
14. S. Xia, M. Qiu, L. Yu, F. Liu, H. Zhao, *Corros. Sci*. 50 ( 2008) 2021.
15. S. John, M. Kuruvilla, A. Joseph, RSC Adv. doi: 10.1039/c3ra40922h.
16. 16 N. Kovacevic, A. Kokalj, *Corros. Sci*. 53 (2011) 909.
17. P.M. Niamien, F.K. Essy, A. Trokourey, A. Yapi, H.K. Aka, D. Diabate, *Mater. Chem. Phys.* 136 (2012) 59.
18. O. L. Humenyuk, O. I. Syza, O. M. Krasovs'kyi, *Mater. Sci*. 43(1) (2007) 85.
19. J. Aljourani, K. Raeissi, M.A. Golozar, *Corros. Sci*. 51 (2009) 1836.
20. N. Kovacevic, A. Kokalj, *Mater. Chem. Phys.* 137 (2012) 331.
21. S. Sun, Y. Geng, L. Tian, S. Chen, Y. Yan, S. Hu, *Corros. Sci.* 63 (20120 140.
22. C. Lee, W. Yang, R.G Parr, *Phys. Rev.* B37 (1988) 785.
23. M.J. Frisch, G.W. Trucks, H.B. Schlegel, G.E. Scuseria, M.A. Robb, J.R. Cheeseman Jr., J.A. Montgomery, T. Vreven, K.N. Kudin, J.C. Burant, J.M. Millam, S.S. Iyengar, J. Tomasi, V. Barone, B. Mennucci, M. Cossi, G. Scalmani, N. Rega, G.A. Petersson, H. Nakatsuji, M. Hada, M. Ehara, K. Toyota, R. Fukuda, J. Hasegawa, M. Ishida, T. Nakajima, Y. Honda, O. Kitao, H. Nakai, M. Klene, X. Li, J.E. Knox, H.P. Hratchian, J.B. Cross, V. Bakken, C. Adamo, J. Jaramillo, R. Gomperts, R.E. Stratmann, O. Yazyev, A.J. Austin, R. Cammi, C. Pomelli, J.W. Ochterski, P.Y. Ayala, K. Morokuma, G.A. Voth, P. Salvador, J.J. Dannenberg, V.G. Zakrzewski, S. Dapprich, A.D. Daniels, M.C. Strain, O. Farkas, D.K. Malick, A.D. Rabuck, K. Raghavachari, J.B. Foresman, J.V. Ortiz, Q. Cui, A.G. Baboul, S. Clifford, J. Cioslowski, B.B. Stefanov, G. Liu, A. Liashenko, P. Piskorz, I. Komaromi, R.L. Martin, D.J. Fox, T. Keith, M.A. Al-Laham, C.Y. Peng, A. Nanayakkara, M. Challacombe, P.M.W. Gill, B. Johnson, W. Chen, M.W. Wong, C. Gonzalez, J.A. Pople, Gaussian 03W, Gaussian Inc., Wallingford CT, 2004.
24. Materials Studio. Revision 6.0. San Diego, USA: Accelrys Inc., 2011.
25. E.E. Oguzie, Y. Li, S.G. Wang, F. Wang, *RSC Adv*. 1 (2011) 866.
26. E. E. Oguzie, C. B. Adindu, C. K. Enenebeaku, C. E. Ogukwe, M. A. Chidiebere, K. L. Oguzie, *J. Phy. Chem. C* 116 (2012) 13603.
27. M. A. Chidiebere, C. E. Ogukwe, K. L. Oguzie, C. N. Eneh, E. E. Oguzie, *Ind. Eng. Chem. Res.* 51 (2012) 668.
28. I. B. Obot, E. E. Ebenso, M.M. Kabanda, *J. Environ. Chem. Eng.* 1(3) (2013) 431.
29. F. Zhang, Y. Tang, Z. Cao, W. Jing, Z. Wu, Y. Chen, *Corros. Sci*. 61 (2012) 1-9.
30. S. M. Anser, R. Haputhanthri, B. Edmonds, D. Liu, L. Yu, A. Sygula, D. Zhang, *J. Phys. Chem. C.* 115 (2011) 653.
31. K. Ravikumar, K. C. Mohan, M. Bidyasagar, G.Y.S.K. Swamy, *J. Chem. Cryst*. 25(6) (1995) 325.
32. P. Udhayakala, A. Jayanthi, T.V. Rajendiran, S. Gunasekaran, *Res. Chem. Intermed*. Doi: 10.1007/s11164-012-0603-0.
33. A.Y. Musa, R.T.T. Jalgham, A. B. Mohamad, *Corros. Sci*. 56 (2012) 176.
34. I. B. Obot, N. O. Obi-Egbedi, A.O. Eseola, *Ind. Eng. Chem. Res*. 50 (2011) 2098.
35. A. Aytac, S. Bilgic, G. Gece, N. Ancin, S.G. Oztas, *Mater. Corros.* 63 (8) (2012) 729.
36. X. Li, S. Deng, H. Fu, T. Li, *Electrochim. Acta* 54 (2009) 4089.
37. H. Jafari, I. Danaee, H. Eskandari, M. RashvandAvei, *Ind. Eng. Chem. Res*. 52 (2013) 6617.
38. H. Tanak, Y. Koysal, S. Isik, H. Yaman, V. Ahsen, *Bull. Korean Chem. Soc.* 32(2) (2011) 673.
39. R. S. Oguike, A. M. Kolo, A. M. Shibdawa, H. A. Gyenna, *ISRN Physical Chem*. (2013) dx.doi.org/10.1155/2013/175910.

40. S. John, J. Joy, M. Prajila, A. Joseph, *Mater. Corros.* 62 (2011) 1031-1041.
41. F. Wang, G. Zhan, Y. Jiang, J. Guo, Z. Yin, R. Feng, *J. Mol. Model* (2013). doi: 10.1007/s00894-013-1843-7.
42. E. E. Oguzie, Z. O. Iheabunike, K. L. Oguzie, C. E. Ogukwe, M. A. Chidiebere, C. K. Enenebeaku, C. O. Akalezi, *J. Dispersion Sci. Tech.* 34 (2013) 516.